Inorganic Chemistry

Article

pubs.acs.org/IC

Design and Syntheses of Electron-Transfer Photochromic Metal–Organic Complexes Using Nonphotochromic Ligands: A Model Compound and the Roles of Its Ligands

Cui-Juan Zhang, Zi-Wei Chen, Rong-Guang Lin, Ming-Jian Zhang, Pei-Xin Li, Ming-Sheng Wang,* and Guo-Cong Guo*

State Key Laboratory of Structural Chemistry, Fujian Institute of Research on the Structure of Matter, Chinese Academy of Sciences, Fuzhou, Fujian 350002, People's Republic of China

Supporting Information

ABSTRACT: The model compound $[Zn(HCOO)_2(4,4'\text{-bipy})]$ (**1**; 4,4′-bipy = 4,4′-bipyridine) is selected in this work to demonstrate the effectiveness of our previously proposed design strategy for electron-transfer photochromic metal–organic complexes. The electron-transfer photochromic behavior of **1** has been discovered for the first time. Experimental and theoretical data illustrate that the photochromism of **1** can be attributed to the electron transfer from formato to 4,4′-bipy and the formation of a radical photoproduct. The electron transfer prefers to occur between formato and 4,4′-bipy, which are combined directly by the Zn(II) atoms. A high-contrast (up to 8.3 times) photoluminescence switch occurs during the photochromic process. The similarity of photochromic behaviors among **1** and its analogues as well as viologen compounds has also been found. Photochromic studies of this model compound indicate that new electron-transfer photochromic metal–organic complexes can be largely designed and synthesized by the rational assembly of nonphotochromic electron-donating and electron-accepting ligands.

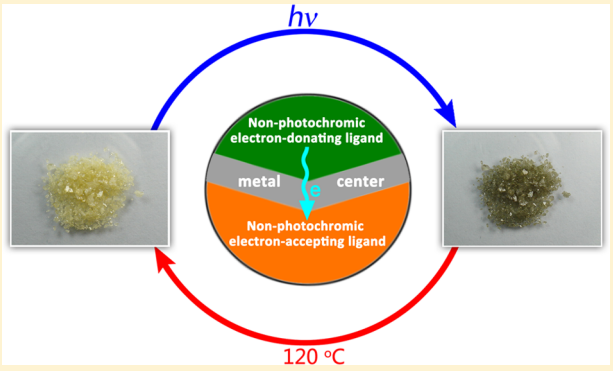

INTRODUCTION

A great number of photochromic materials, with appealing applications for smart windows,[1] photomasks,[2] optical data storage,[3] etc., have been discovered and studied in depth.[4] However, their performances and costs still have to be addressed before they are widely accepted by the market. Exploring new families of photochromic species may offer new opportunities to obtain cost-effective photochromic materials, rather than improving the existing photochromic materials. We and the Wu group have developed a new class of electron-transfer photochromic compounds by the coordination approach.[5] They contain no traditional electron-transfer photochromic units, such as viologens and polyoxometalates of VIB metals, and generally undergo photochromism at room temperature. Ligand-localized (ligand to ligand or intraligand) electron transfer and the formation of radical photoproducts are responsible for their photochromism. We have previously proposed that amines, halides, carboxylate, sulfonate, hydroxyl, sulfhydryl, etc. are candidates for electron donors while π-conjugated groups with electron-withdrawing substituents and high degrees of conjugation are preferable as electron acceptors to trap and stabilize the received electrons.[6] The Fu and Dong groups have successfully synthesized new electron-transfer photochromic coordination compounds using nonphotochromic ligands with the aforementioned groups.[7] Such a photochromic family should be able to be largely expanded because of the diversity of nonphotochromic electron donors and electron acceptors.

To further demonstrate our proposition, the roles of ligands need to be uncovered clearly. The electron-transfer photochromic compounds reported by us as well as the Wu and Fu groups[5,7b] have complex components. For example, $[Cd_2(ic)(mc)(4,4'\text{-bipy})_3]_n{\cdot}4nH_2O$ (ic = itaconate, mc = mesaconate, 4,4′-bipy = 4,4′-bipyridine) has three kinds of organic ligands and lattice water molecules.[5a] Such a complicated structure is not easy for one to distinguish exactly which is the electron-donating ligand and which is the electron-accepting ligand. The components in another example documented by the Dong group are simple, but the roles of the ligands were not completely analyzed.[7a] To understand fully the roles of the ligands, we chose the known 3-D metal–organic framework $[Zn(HCOO)_2(4,4'\text{-bipy})]$ (**1**; Figure 1) as a research target in this work.[8] One reason is that its composition is simple. Its crystallographically independent unit contains only half of one Zn atom, one formato group, and half of a 4,4′-bipy ligand,

Received: August 27, 2013
Published: December 23, 2013

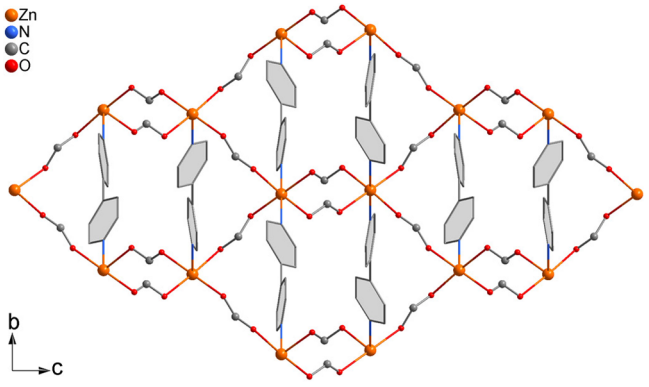

Figure 1. Crystal structure of **1** viewed along the *a* axis. H atoms are not shown for clarity. Note that the crystal structure of **1** has been fully characterized by other groups.[8]

bearing no guest molecules and multiple potential electron donors or acceptors. Another reason is that the presence of the Zn center facilitates the formation of light-colored crystalline samples, which favors the so-called "positive photochromism".[4] Herein, we report its photochromic behavior and the role of each ligand.

RESULTS AND DISCUSSION

Synthesis. Compound **1** was previously synthesized either by the solvothermal reaction of ZnO, HCOOH, and 4,4′-bipy in a water/DMF mixture[8a] or by the reflux reaction of $Zn(CH_3COO)_2{\cdot}4H_2O$, sodium hydrogen 3-sulfobenzoate, and 4,4′-bipy in a water/DMF mixture.[8b] In this work, the synthesis of **1** was simplified by the direct reaction of $Zn(HCOO)_2{\cdot}2H_2O$ and 4,4′-bipy in a water/ethanol mixture at room temperature. Compound **1** has been reported to crystallize in the chiral space group $P4_12_12$[8b] or $P4_32_12$.[8a] The chirality should have less impact on the photochromism of **1**; therefore, we did not separate the as-synthesized single crystals into different chiralities. The phase purity of all crystalline samples used in this work was demonstrated by powder X-ray diffraction (PXRD) determinations (Figure S1, Supporting Information) and elemental analyses in advance.

Photochromism. The photochromic behavior of **1** has never been reported. We found that the pale yellow crystalline sample of **1** turned olive green when illuminated by a 300 W Xe lamp under ambient conditions (Figure 2). The photoresponse range of **1** is ∼260−360 nm, wherein the optimal wavelength is around 300 nm. Such a wavelength-dependence character

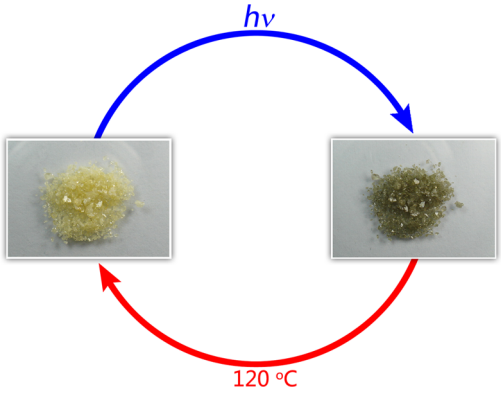

Figure 2. Photochromism of **1**.

demonstrates that the coloration proceeds through a photon mode instead of a photothermal fashion. The photoproduct can be kept in the dark at room temperature for more than 10 months but was easily bleached by annealing at 120 °C for 2 h. Photobleaching is not successful using visible light, as is the case for most electron-transfer photochromic species.[9] Coloration and decoloration of **1** can occur either in air or under vacuum, precluding the action of water and O_2. These coloration−decoloration processes can be repeated at least 10 times. As depicted in Figures S1 and S2 (Supporting Information), the crystal structure and the ligands of **1** experience no clear change during the coloration process.

Diffuse reflectance (DR) analyses clearly demonstrated the photochromic behavior of **1**. After irradiation for 3 min using the Xe lamp, three obvious absorption bands centered at ∼385, 495, and 597 nm, respectively, appeared in the DR spectrum of **1** (Figure 3). These bands became stronger with an increase of

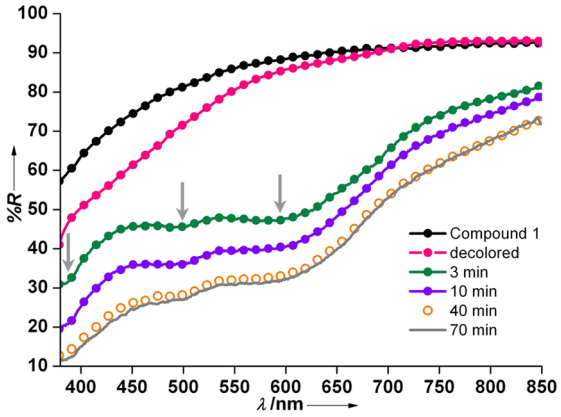

Figure 3. DR spectra of **1**. The gray arrows denote the new absorption bands.

illumination time but had no further clear variation when the sample was irradiated beyond 40 min. They disappeared after decoloration of the sample.

Photochromic Mechanism. The two starting materials, $Zn(HCOO)_2{\cdot}2H_2O$ and 4,4′-bipy, do not show a color change when irradiated for 70 min by the Xe lamp. DR analyses also verify that they do not produce new clear absorption peaks in the wavelength range of visible light (Figure S3, Supporting Information). Therefore, the photochromism of **1** results from the synergetic action between zinc formate and 4,4′-bipy.

The PXRD and IR data, shown in Figures S1 and S2 (Supporting Information), illustrated that the photochromism of **1** is not the result of photoinduced isomerization or photolysis. Thus, the photochromism of **1** very probably originates from an electron-transfer process. This was confirmed by electron spin resonance (ESR) studies (Figure 4). Before irradiation, the crystalline sample of **1** had no ESR signals. After coloration, one single-line signal at $g = 2.0034$ emerged. The zinc atom can be excluded as a paramagnetic center because Zn^{I} and Zn^{III} atoms are unstable in this case and also the ESR spectrum of Zn^{I} has been reported to exhibit anisotropy.[10] This g value is very close to that of a free electron (2.0023), indicating that the paramagnetic center of the colored sample should be a radical. The radical signal disappears again when the sample is thermally bleached.

X-ray photoelectron spectroscopy (XPS) measurements were performed to probe the origin of radicals. As illustrated in

dx.doi.org/10.1021/ic402182j | Inorg. Chem. 2014, 53, 847−851

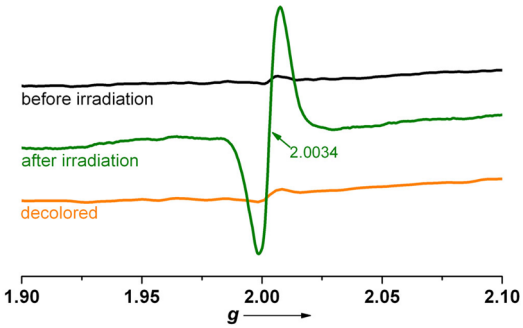

Figure 4. ESR spectra of **1**. The small signal around g = 2.00 for the sample before irradiation was caused by unexpected light during sample handling and ESR measurements.

Figure 5, core-level spectra of both Zn $2p_{3/2}$ and C 1s are almost the same after UV irradiation. However, the variation of

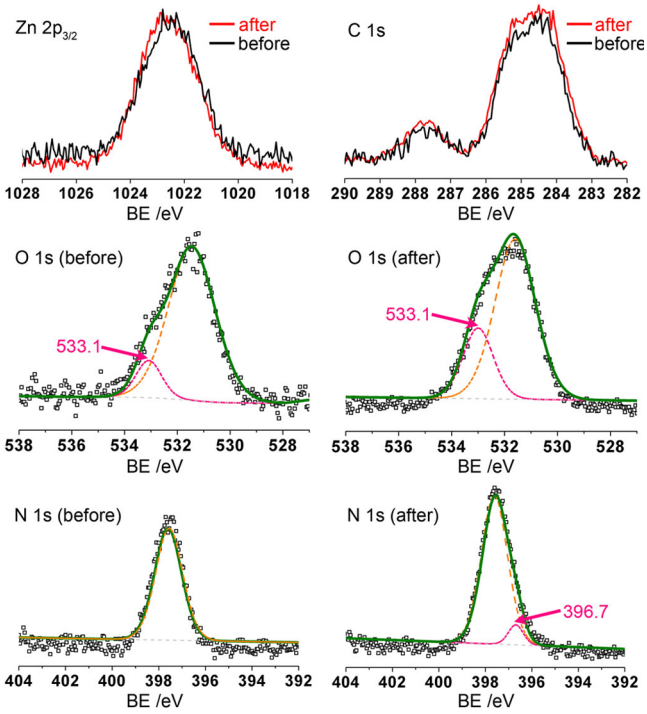

Figure 5. XPS core-level spectra of **1** before and after irradiation. The pink and orange dashed lines depict the resolved peaks, the sum of which is shown using green solid lines.

those of O 1s and N 1s is discernible. Before irradiation, the O 1s core-level spectrum can be fitted to one major peak at 531.5 eV and a weak peak at 533.1 eV. The latter should result from irradiation of unexpected light during sample handling and XPS measurements, because it is significantly enhanced after UV irradiation. The appearance of such a peak means that the formato group loses electrons. As for N 1s, its core-level spectrum contains one major peak at 397.6 eV before irradiation. After irradiation, a new peak emerges at a position with a lower binding energy (396.7 eV), suggesting that the 4,4′-bipy ligand receives electrons. Thus, the radicals should originate from formato → 4,4′-bipy electron transfer on the basis of the XPS data.

To further elucidate the electron-transfer process, total and partial densities of states (DOS) of **1** were calculated on the basis of density functional theory (DFT) using a plane-wave expansion of the wave functions. As shown in Figure 6, the

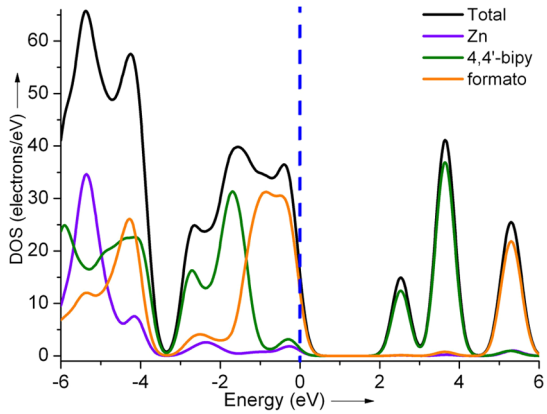

Figure 6. Total and partial DOS of **1**. The Fermi level is set at 0 eV.

valence bands close to the Fermi level (set at 0 eV) are mainly dominated by p−π orbitals of the formato and 4,4′-bipy ligands, while the bottom of the conduction bands is mostly contributed by p−π* antibonding orbitals of the 4,4′-bipy ligands. As mentioned above, the 4,4′-bipy ligand does not possess photochromic behavior. Therefore, this theoretical result demonstrates again that the photochromism of **1** is caused by photoinduced formato → 4,4′-bipy electron transfer.

DR studies revealed that $Zn(HCOO)_2{\cdot}2H_2O$ and 4,4′-bipy have very weak and intense absorptions around 300 nm, respectively (Figure S4, Supporting Information). In addition, the DR spectra of **1** and 4,4′-bipy are very similar. Therefore, the photoexcitation of **1** first happens to 4,4′-bipy, and then the electron from the formato ligand migrates to 4,4′-bipy. It has been well established that electron transfer can occur by through-bond or through-space paths.[11] For **1**, the electron donor (formato) and electron acceptor (4,4′-bipy) are jointed by either dative bonds or weak C−H···N and C−H···O hydrogen bonds (Figure 7). These bonds offer the opportunities for both through-bond and through-space electron transfer, respectively. As shown in Figure 7, the C2−H2A···O2, C5−H5A···O2, C5−H5A···O1, and C1−H1A···N1 hydrogen bonds are clearly shorter than the other bonds. Moreover, the through-bond path via the two metal-mediated dative bonds is undoubtedly the shortest. Thus, the electron transfer prefers to occur between formato and 4,4′-bipy, which are combined directly by the Zn(II) atoms. The best electron-transfer direction goes from the formato ligand with the C1 atom to the 4,4′-bipy ligand with the C2 atom because of the coexistence of the shortest through-bond and through-space paths.

Photochromism and photoluminescence (PL) are nonradiative and radiative processes, respectively. An in situ PL study shows that compound **1** has a broad emissive band upon excitation by 300 nm UV light, which is located in the optimal photoresponse range for the photochromism of **1** (Figure 8). The PL intensity goes down dramatically with an increase of irradiation time and reaches ∼12% of the starting value after illumination for 40 min. These results reveal that PL is a competitive photophysical process for the photochromism of **1**.

The absorption peak of formate radicals falls in the UV range;[12] therefore, the three absorption bands that appear in the visible light range of the photoproduct (Figure 3) are

dx.doi.org/10.1021/ic402182j | Inorg. Chem. 2014, 53, 847−851

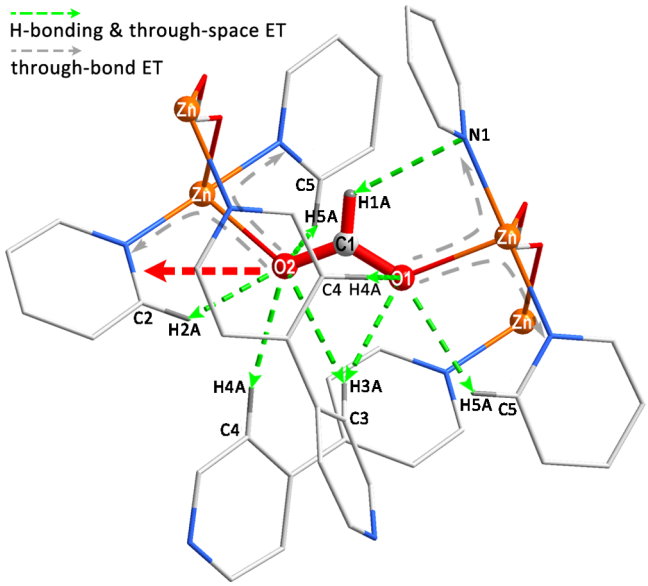

Figure 7. Photoinduced electron-transfer (ET) paths of **1**. The red arrow indicates the best ET direction. Separations (Å) and angles (deg) for bonds: Zn−N = 2.112(2); Zn−O1 = 2.184(2); Zn−O2 = 2.179(2); C2···O2 = 3.080(4), ∠C2−H2A···O2 = 125.3(2); C3···O1 = 3.561(4), ∠C3−H3A···O1 = 154.9(2); C3···O2 = 3.854(4), ∠C3−H3A···O2 = 156.7(2); C4···O1 = 3.688(4), ∠C4−H4A···O1 = 133.2(2); C4···O2 = 3.407(4); ∠C4−H4A···O2 = 162.8(2); C5···O1 = 3.139(4), ∠C5−H5A···O1 = 114.5(2); C5···O2 = 3.208(4), ∠C5−H5A···O2 = 102.4(2); C1···N1 = 3.135(4), ∠C1−H1A···N1 = 123.1(2).

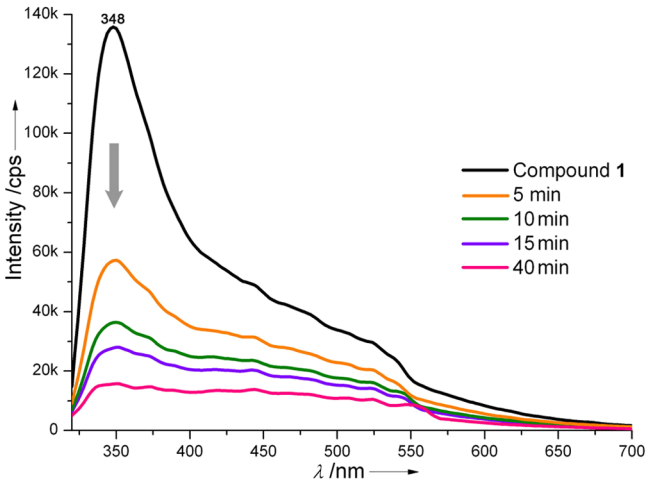

Figure 8. Irradiation time-dependent PL spectra of **1** (λ_{ex} 300 nm).

attributed to the 4,4′-bipy radicals. It should be noted that absorption bands of radical photoproducts for **1** and its analogues[5,7] are similar to those for viologens.[13] In addition, the quenching of PL after irradiation can be found in the analogues of **1**[5b,7b] and viologen-based compounds.[14] We infer that the [Zn^{II}-4,4′-bipy-Zn^{II}] components in **1** and its analogues[5,7a] play the same role as [R-4,4′-bipy-R′] (R, R′ = H, alkyl) units in viologen-based photochromic compounds. To demonstrate this point, theoretical calculations on electronic structures will be necessary in the future. If this is true, then compound **1** and its analogues can be viewed as a class of "metalloviologen" compound.

This work does not focus on the roles of metal centers on photochromism. Their importance at least includes the following two aspects. First, their coordination not only increases the contact between electron donors and acceptors, which facilitates the electron transfer, but also offers through-bond electron-transfer paths. Second, these centers enhance the electron affinity of electron acceptors, which favors the stability of radicals and then the formation of a long-lived charge-separated state. Only the elements Zn, Cd, and Pb, to the best of our knowledge, have been used to construct the new class of electron-transfer photochromic compounds.[5,7] The impact of different metal centers on photochromism remains unexplored.

CONCLUSION

This work has revealed the photochromic properties of **1**, a model compound selected according to our previously proposed design strategy for electron-transfer photochromic metal−organic complexes. Experimental and theoretical data illustrate that the photochromism of **1** can be attributed to formato → 4,4′-bipy electron transfer and the formation of a radical photoproduct. The electron transfer prefers to occur between formato and 4,4′-bipy, which are combined directly by the Zn(II) atoms. A high-contrast (up to 8.3 times) PL switch occurs during the photochromic process. The similarity of photochromic behaviors among **1** and its analogues as well as viologen compounds has also been found. Photochromic studies of this model compound have demonstrated the effectiveness of our proposed strategy to develop new electron-transfer photochromic metal−organic complexes.

EXPERIMENTAL SECTION

Materials. $Zn(HCOO)_2{\cdot}2H_2O$, 4,4′-bipy, and absolute ethanol in AR grade were purchased commercially and used without further purification. Water was deionized and distilled before use.

Physical Measurements. The elemental analyses of C, H, and N were measured on an Elementar Vario EL III microanalyzer. A PLS-SXE300C 300 W xenon lamp system equipped with an IR filter was used to prepare colored samples for FT-IR, DR, PXRD, ESR, and XPS studies, and the distances between these samples and the Xe lamp were around 45 cm. The FT-IR spectra were recorded on a PerkinElmer Spectrum One FT-IR spectrometer using KBr pellets. The DR spectra were recorded on a PerkinElmer Lambda 900 UV/vis/near-IR spectrophotometer equipped with an integrating sphere. $BaSO_4$ plates were used as a reference (100% reflection), on which the finely ground powder of the sample was coated. The PXRD patterns were collected with a Rigaku MiniFlex II diffractometer powered at 30 kV and 15 mA for Cu Kα (λ = 1.54056 Å). The simulated pattern was achieved using the Mercury Version 1.4 software (http://www.ccdc.cam.ac.uk/products/mercury/) and the reported single-crystal X-ray diffraction data. The ESR spectra were recorded at X-band frequency (9.867 GHz) on a Bruker ELEXSYS E500 spectrometer. The XPS studies were performed with a ThermoFisher ESCALAB250 X-ray photoelectron spectrometer (powered at 150 W) using Al Kα radiation (λ = 8.357 Å). To compensate for surface charging effects, all XPS spectra were referenced to the C 1s neutral carbon peak at 284.6 eV. The in situ PL determination was conducted on a single-grating Edinburgh EI920 fluorescence spectrometer equipped with a 450 W Xe lamp and a R928P PMT detector. All of these measurements, except for elemental analyses, were carried out at room temperature.

Synthesis of [$Zn(HCOO)_2$(4,4′-bipy)] (1). This compound has been reported previously.[8] In this work, its single crystals were grown by slow evaporation of a solution of $Zn(HCOO)_2{\cdot}2H_2O$ (0.5 mmol, 96 mg) and 4,4′-bipy (0.5 mmol, 78 mg) in 20 mL of a water/ethanol (4/1 v/v) mixture. Yield: >80%. Anal. Calcd for $C_{12}H_{10}N_2O_4Zn$: C, 46.26; H, 3.23; N, 8.99. Found: C, 46.13; H, 3.17; N, 9.01.

dx.doi.org/10.1021/ic402182j | Inorg. Chem. 2014, 53, 847−851

Computational Details. The calculation model was built directly from the single-crystal X-ray diffraction data of **1**.[8a] Plane wave-based DFT calculations of the total and partial densities of states of **1** were performed using the Cambridge Sequential Total Energy Package (CASTEP) code.[15] The exchange-correlation energy was described by the Perdew–Burke–Eruzerhof (PBE) functional within the generalized gradient approximation (GGA).[16] The norm-conserving pseudopotentials were chosen to modulate the electron–ion interaction.[17] The orbital electrons of C $2s^2 2p^2$, H $1s^1$, N $2s^2 2p^3$, O $2s^2 2p^4$, and Zn $3d^{10} 4s^2$ were treated as valence electrons. The number of plane waves included in the basis was determined by a cutoff energy of 750 eV, and the numerical integration of the Brillouin zone was performed using a 2 × 2 × 1 Monkhorst–Pack *k*-point sampling. Other parameters used in the calculations were set by the default values of the CASTEP code.

■ ASSOCIATED CONTENT

Supporting Information

Figures giving PXRD patterns of **1**, IR spectra of **1** before and after irradiation under ambient conditions, DR spectra of $Zn(HCOO)_2 \cdot 2H_2O$ and 4,4'-bipy before and after irradiation for 70 min, and a comparison of the DR spectra of $Zn(HCOO)_2 \cdot 2H_2O$, 4,4′-bipy, and **1**. This material is available free of charge via the Internet at http://pubs.acs.org.

■ AUTHOR INFORMATION

Corresponding Author

*E-mail: mswang@fjirsm.ac.cn (M.-S.W.), gcguo@fjirsm.ac.cn (G.-C.G.). Fax: +86-591-8371-4946.

Notes

The authors declare no competing financial interest.

■ ACKNOWLEDGMENTS

We gratefully acknowledge financial support by the NSF of China (21373225, 21101152, 21221001, 21271042) and the NSF for Distinguished Young Scholars of Fujian Province (2011J06006).

■ REFERENCES

(1) Bechinger, C.; Ferrere, S.; Zaban, A.; Sprague, J. *Nature* **1996**, *383*, 608–610.
(2) Andrew, T. L.; Tsai, H. Y.; Menon, R. *Science* **2009**, *324*, 917–921.
(3) Kawata, S.; Kawata, Y. *Chem. Rev.* **2000**, *100*, 1777–1788.
(4) Bouas-Laurent, H.; Dürr, H. *Pure Appl. Chem.* **2001**, *73*, 639–665.
(5) (a) Wang, M.-S.; Guo, G.-C.; Zou, W.-Q.; Zhou, W.-W.; Zhang, Z.-J.; Xu, G.; Huang, J.-S. *Angew. Chem., Int. Ed.* **2008**, *47*, 3565–3567. (b) Zhu, Q.-L.; Sheng, T.-L.; Fu, R.-B.; Hu, S.-M.; Chen, L.; Shen, C.-J.; Ma, X.; Wu, X.-T. *Chem. Eur. J.* **2011**, *17*, 3358–3362.
(6) Wang, M.-S.; Xu, G.; Zhang, Z.-J.; Guo, G.-C. *Chem. Commun.* **2010**, *46*, 361–376.
(7) (a) Jiang, Y.-Y.; Ren, S.-K.; Ma, J.-P.; Liu, Q.-K.; Dong, Y.-B. *Chem. Eur. J.* **2009**, *15*, 10742–10746. (b) Fu, Z.-Y.; Chen, Y.; Zhang, J.; Liao, S.-J. *J. Mater. Chem.* **2011**, *21*, 7895–7897.
(8) (a) Zhang, D.-Q.; Zhang, W.-H.; Chen, J.-X.; Ren, Z.-G.; Zhang, Y.; Lang, J.-P. *Acta Chim. Sin.* **2005**, *63*, 2089–2092. (b) Miao, X.-H.; Xiao, H.-P.; Zhu, L.-G. *Acta Crystallogr.* **2006**, *E62*, m1756–m1757.
(9) (a) Monk, P. M. S. *The Viologens: Physicochemical Properties, Synthesis, and Application of the Salt of 4,4′-Bipyridine*; Wiley: New York, 1998. (b) He, T.; Yao, J. *Prog. Mater. Sci.* **2006**, *51*, 810–879.
(10) Tian, Y.; Li, G.-D.; Chen, J.-S. *J. Am. Chem. Soc.* **2003**, *125*, 6622–6623.
(11) (a) Kavarnos, G. J.; Turro, N. J. *Chem. Rev.* **1986**, *86*, 401–449. (b) Wasielewski, M. R. *Chem. Rev.* **1992**, *92*, 435–461.
(12) Illés, E.; Takács, E.; Dombi, A.; Gajda-Schrantz, K.; Rácz, G.; Gonter, K.; Wojnárovits, L. *Sci. Total Environ.* **2013**, *447*, 286–292.
(13) (a) Bockman, T. M.; Kochi, J. K. *J. Org. Chem.* **1990**, *55*, 4127–4135. (b) Vermeulen, L. A.; Thompson, M. E. *Nature* **1992**, *358*, 656–658.
(14) (a) Xu, G.; Guo, G.-C.; Guo, J.-S.; Guo, S.-P.; Jiang, X.-M.; Yang, C.; Wang, M.-S.; Zhang, Z.-J. *Dalton Trans.* **2010**, *39*, 8688–8692. (b) Sun, J.-K.; Cai, L.-X.; Chen, Y.-J.; Li, Z.-H.; Zhang, J. *Chem. Commun.* **2011**, *47*, 6870–6872.
(15) Clark, S. J.; Segall, M. D.; Pickard, C. J.; Hasnip, P. J.; Probert, M. J.; Refson, K.; Payne, M. C. *Z. Kristallogr.* **2005**, *220*, 567–570.
(16) Perdew, J. P.; Burke, K.; Ernzerhof, M. *Phys. Rev. Lett.* **1996**, *77*, 3865–3867.
(17) Hamann, D. R.; Schlüter, M.; Chiang, C. *Phys. Rev. Lett.* **1979**, *43*, 1494–1497.